

# High current sensitivity and large magnetoelectric effect in magnetostrictive–piezoelectric concentric ring

Cite as: J. Appl. Phys. **115**, 17A933 (2014); <https://doi.org/10.1063/1.4867227>

Submitted: 19 September 2013 . Accepted: 26 November 2013 . Published Online: 10 March 2014

Chung Ming Leung, Siu Wing Or, and S. L. Ho



View Online



Export Citation



CrossMark

## ARTICLES YOU MAY BE INTERESTED IN

**Multiferroic magnetoelectric composites: Historical perspective, status, and future directions**  
Journal of Applied Physics **103**, 031101 (2008); <https://doi.org/10.1063/1.2836410>

**DC magnetic field sensor based on electric driving and magnetic tuning in piezoelectric/magnetostrictive bilayer**

Journal of Applied Physics **115**, 17E520 (2014); <https://doi.org/10.1063/1.4866516>

**Ring-type electric current sensor based on ring-shaped magnetoelectric laminate of epoxy-bonded  $Tb_{0.3}Dy_{0.7}Fe_{1.92}$  short-fiber/NdFeB magnet magnetostrictive composite and  $Pb(Zr, Ti)O_3$  piezoelectric ceramic**

Journal of Applied Physics **107**, 09D918 (2010); <https://doi.org/10.1063/1.3360349>

Lock-in Amplifiers  
Find out more today



Zurich  
Instruments



# High current sensitivity and large magnetoelectric effect in magnetostrictive–piezoelectric concentric ring

Chung Ming Leung, Siu Wing Or,<sup>a)</sup> and S. L. Ho  
 Department of Electrical Engineering, The Hong Kong Polytechnic University, Hung Hom, Kowloon, Hong Kong

(Presented 5 November 2013; received 19 September 2013; accepted 26 November 2013; published online 10 March 2014)

A magnetostrictive–piezoelectric concentric ring (MPCR) is fabricated, and its current sensitivity and magnetoelectric effect are studied theoretically and experimentally. The MPCR has an inner Tb<sub>0.3</sub>Dy<sub>0.7</sub>Fe<sub>1.92</sub>/NdFeB/epoxy magnetostrictive composite ring with a circumferential magnetization and an internal magnetic biasing bonded concentrically to an outer Pb(Zr, Ti)O<sub>3</sub> piezoelectric ceramic ring with a wall-thickness polarization. The current sensing in the MPCR is based on the direct coupling of vortex magnetic fields generated by current-carrying cables with the magnetoelectric effect in the MPCR structure. The MPCR shows high and linear current sensitivities and magnetoelectric voltage coefficients of 15–17 mV/A and 22–26 mV/Oe in the nonresonance frequency range of 1 Hz–50 kHz, and of 185 mV/A and 277 mV/Oe at the fundamental shape resonance of 96 kHz, for current and vortex magnetic field levels of up to 10 A and 6.7 Oe, respectively. © 2014 AIP Publishing LLC. [<http://dx.doi.org/10.1063/1.4867227>]

Magnetostrictive–piezoelectric laminates, owing to their generally simple fabrication, tailorable properties, and large magnetoelectric (ME) effect enabled by a plate- or disk-shaped configuration as well as a longitudinal, transverse, radial or axial magnetization/polarization arrangement, have evolved into an important type of ME materials for magnetic field sensing over the past decade.<sup>1–4</sup> However, the unidirectional sensing nature of the laminates often restricts them from direct-sensing vortex or rotating magnetic fields such as those generated by current-carrying cables,<sup>5</sup> and so an auxiliary means (e.g., a ferrite core) is required to channel the vortex magnetic fields into unidirectional magnetic fields for the laminates.<sup>5</sup> In this work, we propose a magnetostrictive–piezoelectric concentric ring (MPCR) for direct-sensing of cable currents of up to 10 A amplitude (corresponding to vortex magnetic fields of up to 6.7 Oe) and 125 kHz frequency. The MPCR is formed by concentrically combining a Tb<sub>0.3</sub>Dy<sub>0.7</sub>Fe<sub>1.92</sub>/NdFeB/epoxy magnetostrictive composite ring (MCR) with a Pb(Zr, Ti)O<sub>3</sub> piezoelectric ceramic ring (PCR) to realize the preferred vortex magnetic field sensing mode. The MCR possesses a circumferential magnetization and an internal magnetic biasing while the PCR carries a wall-thickness polarization. In fact, the introduction of the specifically designed three-phase MCR, consisting of [112]-oriented Tb<sub>0.3</sub>Dy<sub>0.7</sub>Fe<sub>1.92</sub> short fibers and NdFeB magnet bars embedded and aligned in a passive epoxy matrix, is to resolve the problems of unidirectional magnetization, external magnetic biasing, mechanical brittleness as well as eddy current-induced heating and bandwidth limitation intrinsic in monolithic Tb<sub>0.3</sub>Dy<sub>0.7</sub>Fe<sub>1.92</sub> rings.<sup>6–8</sup>

Figure 1 illustrates the schematic diagram and photograph of the proposed MPCR with a vortex magnetic field sensing mode configuration. The inner portion of the MPCR is a three-phase MCR of Tb<sub>0.3</sub>Dy<sub>0.7</sub>Fe<sub>1.92</sub> short fibers, NdFeB

magnet bars, and Araldite LY5210/HY2954 epoxy matrix while the outer portion is a PCR of Pb(Zr, Ti)O<sub>3</sub>. The MPCR was formed by using the PCR as the mold and preparing the MCR in the PCR mold. In more detail, a Pz27 hard Pb(Zr, Ti)O<sub>3</sub> ring was acquired with dimensions of 11.9 mm outer diameter (2r<sub>p</sub>) × 9.9 mm inner diameter (2r<sub>m</sub>) × 1 mm thickness (t), full fired silver electrodes on the inner and outer circumferential surfaces normal to the wall-thickness (or r-) direction, and an electric polarization (P) along the r-direction. [112]-oriented Tb<sub>0.3</sub>Dy<sub>0.7</sub>Fe<sub>1.92</sub> short fibers of 1–1.5 mm length and 0.8 mm width were cut along the length of a [112]-textured monolithic Tb<sub>0.3</sub>Dy<sub>0.7</sub>Fe<sub>1.92</sub> plate using a wire electrical discharge machining technique. Four pieces of NdFeB magnet bars, each with dimensions of 3.95 mm length (L<sub>b</sub>) × 1 mm width (W<sub>b</sub>) × 1 mm thickness (t) and having the north (N) and south (S) poles normal to its rectangular surfaces of cross-sectional area defined by L<sub>b</sub> × t, were also prepared. In fabrication, the four NdFeB magnet bars were arranged in the 0°, 90°, 180°, and 270° directions in the PCR mold, and a predetermined quantity of Tb<sub>0.3</sub>Dy<sub>0.7</sub>Fe<sub>1.92</sub> short

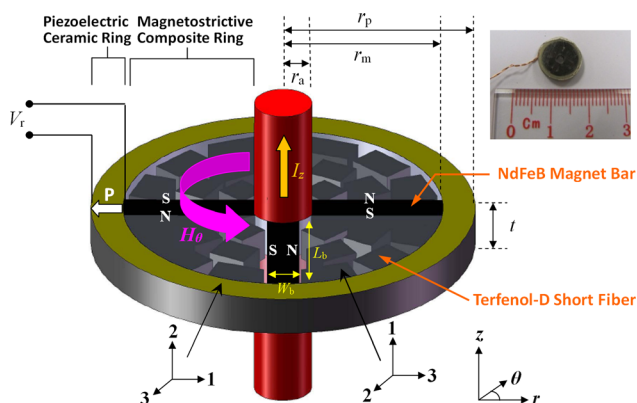


FIG. 1. Schematic diagram and photograph of the proposed MPCR with a vortex magnetic field detection mode configuration.

<sup>a)</sup>Author to whom correspondence should be addressed. Electronic mail: ceswor@polyu.edu.hk.

fibers was placed between the NdFeB magnet bars inside the PCR mold. The dc magnetic field of  $\sim 200$  Oe set up by the NdFeB magnet bars in the circumferential (or  $\theta$ -) direction not only caused the  $\text{Tb}_{0.3}\text{Dy}_{0.7}\text{Fe}_{1.92}$  short fibers to align with the magnetic flux lines and produce short-fiber chains along the  $\theta$ -direction but also imparted a magnetic bias to enhance the magnetostrictive effect in the aligned  $\text{Tb}_{0.3}\text{Dy}_{0.7}\text{Fe}_{1.92}$  short fibers.<sup>7</sup> The predegreased Araldite epoxy was transferred into the PCR mold and degassed again inside the mold. The mold was sealed, and the epoxy was allowed to cure at  $80^\circ\text{C}$  for 9 h. After demolding, a central hole of 2 mm diameter ( $2r_a$ ) was opened in the magnetostrictive composite to form the MCR and so the MPCR structure for cable insertion. It is noted that the MCR was circumferentially magnetized and magnetically biased without the need of an external basing means as in the previous works.<sup>1-4</sup>

The current sensing in the MPCR is essentially based on the direct coupling of vortex magnetic fields generated by current-carrying cables with the ME effect in the MPCR structure. Referring to Fig. 1, when an ac current ( $I_z$ ) is applied to a cable in the axial (or  $z$ -) direction, an ac vortex magnetic field ( $H_\theta$ ) is induced about the length of the cable in the circumferential (or  $\theta$ -) direction in accordance with Ampère's law. Because of the nonuniform distribution of  $H_\theta$  over the volume ( $v_{\text{vol}}$ ) of the MPCR, an average ac vortex magnetic field ( $H_{\theta,\text{avg}}$ ) is detected instead, causing the inner MCR to produce circumferential and also radial motions due to the magnetostrictive effect. As the inner MCR is coupled mechanically to the outer PCR, the magnetostrictive strains will subsequently stress the PCR to generate an ac voltage ( $V_r$ ) across the wall thickness of the PCR in the wall-thickness (or  $r$ -) direction owing to the piezoelectric effect. This mechanically mediated product effect of the magnetostrictive and piezoelectric effects is referred to an extrinsic ME effect.<sup>1-4</sup>

According to Ampère's law, the relation between  $I_z$  and  $H_{\theta,\text{avg}}$  can be written as<sup>5</sup>

$$H_{\theta,\text{avg}} = \frac{1}{v_{\text{vol}}} \int_{r_a}^{r_m} H_\theta d\nu_{\text{vol}} = \frac{I_z}{\pi(r_m + r_a)}. \quad (1)$$

Because the MCR is thin in the thickness (or  $z$ -) direction and is magnetized along the  $\theta$ -direction, the following constitutive piezomagnetic equations are used:<sup>6</sup>

$$S_{3,m} = s_{33}^H T_{3,m} + d_{33,m} H_3, \quad (2a)$$

$$B_3 = d_{33,m} T_{3,m} + \mu_{33}^T H_3, \quad (2b)$$

where  $H_3$  ( $=H_{\theta,\text{avg}}$ ) and  $B_3$  are the magnetic field strength and magnetic induction along the  $\theta$ -direction, respectively;

$T_{3,m}$  and  $S_{3,m}$  are the mechanical stress and strain along the  $\theta$ -direction, respectively;  $\mu_{33}^T$  is the magnetic permeability at constant stress;  $d_{33,m}$  ( $=1.05$  nm/A) is the piezomagnetic strain coefficient; and  $s_{33}^H$  ( $=61.2$  pm<sup>2</sup>/N) is the elastic compliance coefficient at constant magnetic field strength. Since the PCR is also thin in the  $z$ -direction and is finite and polarized in the  $r$ -direction, the following constitutive piezoelectric equations are adopted:<sup>9</sup>

$$S_{1,p} = s_{11}^E T_{1,p} + d_{31,p} E_3, \quad (3a)$$

$$D_3 = \bar{d}_{31,p} T_{1,p} + \epsilon_{33}^T E_3, \quad (3b)$$

where  $E_3$  ( $=E_r$ ) and  $D_3$  are the electric field and electric displacement along the  $r$ -direction, respectively;  $T_{1,p}$  and  $S_{1,p}$  are the mechanical stress and strain along the  $\theta$ -direction, respectively;  $\epsilon_{33}^T$  ( $=1800 \epsilon_0$ ) is the dielectric permittivity at constant stress;  $\bar{d}_{31,p}$  ( $=-170$  pC/N) is the piezoelectric strain coefficient; and  $s_{11}^E$  ( $=17$  pm<sup>2</sup>/N) is the elastic compliance coefficient at constant electric field strength. Assuming a perfect mechanical coupling between the MCR and the PCR such that the mechanical boundaries for stress and strain are  $T_{3,m}(r_m - r_a) + T_{1,p}(r_p - r_m) = 0$  and  $S_{3,m} = S_{1,p}$ , respectively, the following equations are obtained from Eqs. (2a) and (3a), respectively:

$$(r_m - r_a) \left( \frac{\epsilon_{33}^T E_r}{d_{31,p}} \cdot \frac{r_p - r_m}{r_m - r_a} \right) = (r_p - r_m) \left( \frac{\epsilon_{33}^T E_r}{d_{31,p}} \right), \quad (4a)$$

$$s_{33}^H T_{3,m} + d_{33,m} H = s_{11}^E T_{1,p} + d_{31,p} E_3. \quad (4b)$$

For open-circuit condition, Eq. (3b) becomes

$$d_{31,p} \left( -\frac{\epsilon_{33}^T E_r}{d_{31,p}} \right) + \epsilon_{33}^T E_3 = 0. \quad (5)$$

Combining Eqs. (4) and (5), the ME voltage coefficient ( $\alpha_V$ ) of the MPCR is

$$\begin{aligned} \alpha_V &= \frac{dV_r}{dH_{\theta,\text{avg}}} \\ &= \frac{d_{33,m} g_{31,p} (r_m - r_a) (r_p - r_m)}{s_{33}^H (r_p - r_m) + s_{11}^E (r_m - r_a) - d_{31,p} g_{31,p} (r_m - r_a)}. \end{aligned} \quad (6)$$

From Eqs. (1) and (6), the current sensitivity ( $S_I$ ) of the MPCR is

$$S_I = \frac{dV_r}{dI_z} = \frac{dV_r}{dH_{\theta,\text{avg}}} \cdot \frac{dH_{\theta,\text{avg}}}{dI_z} = \alpha_V \cdot \frac{dH_{\theta,\text{avg}}}{dI_z} = \frac{d_{33,m} g_{31,p} (r_m - r_a) (r_p - r_m)}{[s_{33}^H (r_p - r_m) + s_{11}^E (r_m - r_a) - d_{31,p} g_{31,p} (r_m - r_a)] \pi (r_m + r_a)}. \quad (7)$$

With the material properties given above and the geometric parameters described in Fig. 1,  $S_I$  and  $\alpha_V$  of the MPCR are predicted to be 19.3 mV/A [Eq. (7)] and 28.8 mV/Oe [Eq. (6)], respectively, at nonresonance frequencies.

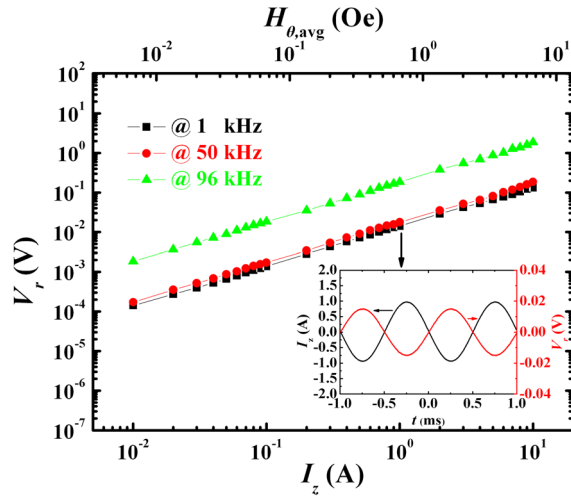


FIG. 2.  $V_r$  output from MPCR over board ranges of  $I_z$  of  $10^{-2}$ –10 A and its associated  $H_{\theta,avg}$  of  $6.7 \times 10^{-3}$ –6.7 Oe at three different  $f$  of 1, 50, and 96 kHz. The inset shows the waveform of  $V_r$ , due to  $I_z$  of 1 A peak at 1 kHz.

The MPCR was inserted in a cable of diameter 1.8 mm (Fig. 1), and the MPCR–cable assembly was placed in an electromagnetic interference-shielded chamber for measurements. Figure 2 plots  $V_r$  output from the MPCR over board ranges of  $I_z$  of  $10^{-2}$ –10 A and its associated  $H_{\theta,avg}$  of  $6.7 \times 10^{-3}$ –6.7 Oe at three different frequencies ( $f$ ) of 1, 50, and 96 kHz. The values of  $H_{\theta,avg}$  are determined using Eq. (1). It is clear that  $V_r$  varies essentially linearly with both  $I_z$  and  $H_{\theta,avg}$  at all  $f$  even at a very small  $I_z$  of 0.01 A. The good linearity between  $V_r$  and  $I_z$ , and also between  $V_r$  and  $H_{\theta,avg}$ , confirms the validity of the proposed working principle. From the slopes of plot,  $S_I$  of the MPCR is determined to be 14.7, 17.2, and 185 mV/A at 1, 50, and 96 kHz, respectively while  $\alpha_V$  is found to be 22, 25.7, and 277 mV/Oe at 1, 50, and 96 kHz, respectively. The measured  $S_I$  and  $\alpha_V$  values at the nonresonance  $f$  of 1 and 50 kHz agree with the predicted  $S_I$  and  $\alpha_V$  values of 19.3 mV/A and 28.8 mV/Oe based on Eqs. (6) and (7), respectively. The significant increase in both  $S_I$  and  $\alpha_V$  at 96 kHz is a result of the fundamental shape resonance of the MPCR to be discussed in Fig. 3. The inset of Fig. 2 shows the waveform of the measured  $V_r$  due to an applied  $I_z$  of 1 A peak at 1 kHz. It is seen that  $V_r$  has a  $180^\circ$  phase reveal with respect to  $I_z$  because the piezoelectric coefficient ( $g_{31,p} = d_{31,p}/\epsilon_{33}^T$ ) in Eq. (7) carries a negative sign.

Figure 3(a) shows  $S_I$  of the MPCR in the  $f$  range of 40 Hz–125 kHz with an  $I_z$  of 1 A applied to the cable. For comparison, a reluctance coil with a turn number of 100 was wrapped around the cable to detect  $I_z$ . It is obvious that  $S_I$  of the MPCR has a reasonably high and flat response to  $f$ , which is 15–17 mV/A, in the range of 1 Hz–50 kHz. A fundamental shape resonance, corresponding to the radial mode of vibration of the MPCR, is observed at 96 kHz with a significantly high  $S_I$  of 185 mV/A. Nevertheless, this suggests that our MPCR has an essentially flat and usable detection bandwidth up to and beyond 50 kHz. For the reluctance coil, its  $S_I$  depends strongly on  $f$  with a typical inductive effect. For  $f$  below 50 Hz, the environmental noise level is larger than the voltage induced by the reluctance coil so that its  $S_I$  value decreases dramatically to  $\sim 7 \mu\text{V/A}$ . To give a physical insight into the resonance effect of the MPCR, Fig. 3(b)

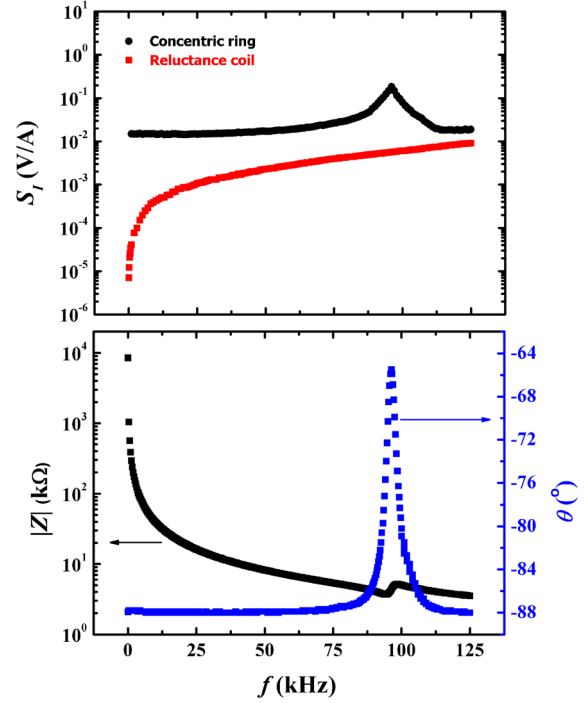


FIG. 3. (a)  $S_I$  of MPCR in the  $f$  range of 1 Hz–125 kHz with  $I_z$  of 1 A applied to the cable.  $S_I$  of a reluctance coil wrapped around the cable is also included. (b)  $|Z|$  and  $\theta$  as a function of  $f$  for MPCR in the 40 Hz–125 kHz range.

shows the electrical impedance ( $|Z|$ ) and phase angle ( $\theta$ ) as a function of  $f$  for the MPCR in the 40 Hz–125 kHz range. A clear electromechanical resonance peak is detected at 96 kHz, which agrees well with the  $S_I$  peak as seen in Fig. 3(a).

We have developed an interesting device to detect vortex magnetic fields generated by current-carrying cables and, hence, currents flowing through the cables based on a MPCR having a circumferential magnetization, a wall-thickness polarization, and an internal magnetic biasing. The results have shown the presence of high and linear  $S_I$  and  $\alpha_V$  of 15–17 mV/A and 22–26 mV/Oe in the nonresonance frequency range of 1 Hz–50 kHz, and of 185 mV/A and 277 mV/Oe at the fundamental shape resonance of 96 kHz, for  $I_z$  and  $H_{\theta,avg}$  levels of up to 10 A and 6.7 Oe, respectively. The simultaneous power supply-free, magnetic bias-free, high-sensitive, and wide-bandwidth natures of our MPCR compared to traditional active current or magnetic field sensors such as Hall sensors make it great potential for real-time, *in-situ* sensing of cable currents.

This work was supported by the Research Grants Council of the HKSAR Government (PolyU 5228/13E) and The Hong Kong Polytechnic University (H-ZG76 and 1-ZV7P).

- <sup>1</sup>M. Fiebig, *J. Phys. D: Appl. Phys.* **38**, R123 (2005).
- <sup>2</sup>Y. M. Jia *et al.*, *J. Appl. Phys.* **101**, 104103 (2007).
- <sup>3</sup>Y. J. Wang *et al.*, *J. Appl. Phys.* **103**, 124511 (2008).
- <sup>4</sup>C. M. Leung *et al.*, *Rev. Sci. Instrum.* **82**, 013903 (2011).
- <sup>5</sup>R. F. Harrington, *Introduction to Electromagnetic Engineering* (Dover, NY, 2003).
- <sup>6</sup>G. Engdahl, *Magnetostrictive Materials Handbook* (Academic, NY, 2000).
- <sup>7</sup>S. W. Or *et al.*, *J. Appl. Phys.* **93**, 8510 (2003).
- <sup>8</sup>S. W. Or *et al.*, *J. Appl. Phys.* **97**, 10M308 (2005).
- <sup>9</sup>T. Ikeda, *Fundamentals of Piezoelectricity* (Oxford University Press, Oxford, 1990).